

Multi-stream Faster RCNN for Mitosis Counting in Breast Cancer Images

Robin Elizabeth Yancey

March 3, 2022

1 Abstract

Mitotic count is a commonly used method to assess the level of progression of breast cancer, which is now the fourth most prevalent cancer. Unfortunately, counting mitosis is a tedious and subjective task with poor reproducibility, especially for non-experts. Luckily, since the machine can read and compare more data with greater efficiency this could be the next modern technique to count mitosis. Furthermore, technological advancements in medicine have led to the increase in image data available for use in training. In this work, we propose a network constructed using a similar approach to one that has been used for image fraud detection with the segmented image map as the second stream input to Faster RCNN [27]. This region-based detection model combines a fully convolutional Region Proposal Network to generate proposals and a classification network to classify each of these proposals as containing mitosis or not. Features from both streams are fused in the bilinear pooling layer to maintain the spatial concurrence of each. After training this model on the ICPR 2014 MITOSIS contest dataset [29], we received an F-measure score of , higher than both the winners score and scores from recent tests on the same data. Our method is clinically applicable, taking only around five min per ten full High Power Field slides when tested on a Quadro P6000 cloud GPU.

2 Introduction

It is estimated that breast cancer incidences will increase by more than 50% by 2030 from 2011 [4]. Mitosis counting is one of the commonly used methods of assessing the level of progression of breast cancer, and is a routine task for every patient diagnosed with invasive cancer [4]. The Nottingham Grading System (NGS) is recommended by various professional bodies internationally (World Health Organization [WHO], American Joint Committee on Cancer [AJCC], European Union [EU], and the Royal College of Pathologists (UK RCPATH) [24]. It says that tubule formation, nuclear pleomorphism, and mitotic index should each be rated from 1 to 3, with the final score ranging between 3 and 9. This is

divided into three grades: Grade 1, score 35, well differentiated; Grade 2, score 67, moderately differentiated; and Grade 3, score 89, poorly differentiated [3]. Although mitotic count is the strongest prognostic value [19], it is tedious and subjective task with poor reproducibility, especially for non-experts [37].

When pathologists need to make this assessment of the tumor, they start by finding the region with the highest proliferative activity. The mitotic count is defined in a region from 10 consecutive high-power fields (HPF) within a space of $2mm^2$. Variation in phase and slide preparation techniques make it possible to misdiagnose. Depending on whether the mitosis is in one of the four main phases: prophase, metaphase, anaphase and telophase the shape of the differs significantly. For example, when in telophase it is split into to separate regions even though they are still one connected mitotic cell. Apoptotic cells (or cells going through preprogrammed cell death) and other scattered pieces of waste on the slides can also easily be confused with mitoses, having a similar dark spotty appearance. The variation in the process of obtaining the slides using different scanners and techniques may also make distinguishing cells difficult. Furthermore, trained pathologists need to examine hundreds of high power fields (HPF) of histology images, meaning biopsies can take up to ten days before the patient receives results [25]. The increasing numbers of breast cancer incidences calls for a more time and cost efficient method of prognosis, which could later even help to provide care to impoverished regions. Automatic image analysis has recently proven to be a possible solution, with inter-observer agreement when tested against the human judgement [37].

Due to the recent progress in digital medication, a large amount of of data has became available for use in the medical studies. Machine learning has helped to discover new characteristics of cancer mutations by sorting through more image data than humanly possible and by simultaneously analyzing all of the millions of image pixels undetectable to the human eye. For example, in the field of histopathology machine learning algorithms have been used for analysis of scanned slides to assist in tasks including diagnosis [13]. The use of computing in image analysis may reduce variability in interpretation, improve classification accuracy, and provide clinicians (or those in training) with a second opinion [13].

Deep learning often outperforms traditional methods such as use the of hand-crafted features alone since features and classifiers are simultaneously optimized. This is because pathological images are texture-like in nature, making them ideal task for CNN to learn with their shift invariance and pooling operations. They are also well-suited to learn high level features such as mitotic count, which is likely what made CNN methods winners of the MITOS-ATYPIA 2012 challenge [30], the MITOS-ATYPIA 2014 challenge [29], and the AMIDA 2013 challenge [38] [25]. On the other hand, CNN lacks cell level supervision and often requires limiting the size of the input image so that sub-image features can be learned.

Faster-RCNN [27] is a newer more sophisticated model that combines a CNN with a Region Proposal Network (RPN) to classify sub-image region proposals, while using a sliding window to produce spatial coordinates for bounding boxes associated with certain classes. This technique was used to improve upon current

methods of object detection in both speed and accuracy. Consequently, the novel idea to apply these object detection networks to detect non-objects such as mitosis detection by [25] resulted in an F-score of 0.955 (6.22% more accurate than the previous score of 0.900 achieved by the model proposed by [31] on the above challenge datasets when trained on all 3 datasets.)

The classification models used for image tampering detection are highly similar to that of mitosis detection in HPFs in that their purpose is to localize regions of interest with different textures (indistinguishable to the human eye). Another application of this network to non-objects was a bilinear version of Faster RCNN to detect image tampering in [45] which largely outperformed an individual stream as well as many current 'state-of-the-art' methods on standard image manipulation datasets. The purpose of the RGB (red, green, blue color scale) stream is to find regions of high color contrast difference, while the purpose of the second stream (the noise stream) is to extract regions with noise inconsistency. Region proposals are taken from the RGB stream alone, but features from both streams are fused in the bilinear pooling layer to maintain the spatial concurrence of each.

Even higher accuracy was obtained by applying an algorithm for image tampering segmentation as input to the second stream in place of the noise map [43] [44], because segmentation achieves a higher contrast between textures. Histopathological image segmentation is also commonly used to extract and highlight objects of interest from the background of the image (with different textures) for further identification. Some of the methods used for mitosis counting or cancer cell identification have included thresholding (using Fourier descriptors, wavelets or Otsu), edge detection (using Canny and Sobel filters), or clustering (such as k-means, mean-shift, and K-nn) [16] [35]. Since the segmented image map can significantly improve classification accuracy in image tampering by applying it as input to a second stream of the Faster RCNN model, it also can improve mitosis detection accuracy. In this work, classification accuracy is improved by applying a segmented image map as input to a second stream of the model.

3 Related Work

Techniques used to count mitosis in HPF images typically fall into the category of those based on handcrafted features or CNN features. The handcrafted features are explicit characteristics of mitosis designed based on the histopathologists knowledge of the morphology, intensity and texture. Current methods also often fall into the category of considering mitosis detection as a classification problem or as a semantic segmentation problem. When it is framed as a classification problem each of the regions are usually classified as containing a mitosis or no-mitosis using a sliding window across the image. On the other hand, when it is framed as a segmentation problem a fully connected network is often used to give each pixel in the image a given intensity where a threshold determines whether or not it is a pixel contained in a mitosis. A number

of contests have been held to motivate groups to compete to design the best computer aided detection system (where the mitosis is mapped according to pixel intensity.) These include the 2012 International Conference on Pattern Recognition (ICPR12) [30] Mitosis Detection Contest, the Assessment of Mitosis Detection Algorithms 2013 Challenge (AMIDA13) [38] and the 2014 ICPR Mitosis Detection Challenge (MITOS-ATYPIA-14) [29].

There have been a number of other handcrafted feature methods tested on ICPR 2012. (Liu et al., 2010) proposed a two part mitosis event detection technique using hidden conditional random field, where candidate spatiotemporal sub-regions were segmented by image pre-conditioning and volumetric segmentation [21]. (Huh et al. 2011), use phase-contrast microscopy images consisting of three steps: candidate patch sequence construction, visual feature extraction, and identification of mitosis occurrence/temporal localization of birth event [11]. (Khan et al., 2012) modeled mitosis intensities by a gamma distribution and those from non-mitotic regions by a gaussian distribution [12]. (Sommer et al., 2012) trained a pixel-wise classifier to segment candidate cells, which are classified into mitotic and non-mitotic cells based on object shape and texture [33]. (Huang & Lee, 2012) propose an extension of a generic ICA, focusing the components of differences between the two classes of training patterns [10]. (Veta et al., 2013) extracts image segmentation with the Chan-Vese level set method and classifies potential objects based on a number of size, shape, color and texture features [36]. (Tek et al. 2013) use an ensemble of cascade adaboosts classified mainly by a shape-based feature, which counted granularity and red, green, and blue channel statistics [34]. There have been a few groups using handcrafted-features to report F-measure scores close to the highest score achieved in the ICPR 2012 contest. For example, (Irshad, 2013) proposed a method where cells are segmented by extracting various color channel features followed by a candidate detection that included Laplacian of Gaussian, thresholding, and morphological operations, achieving an F-measure score of 0.72 on the ICPR 2012 dataset. (Irshad et al., 2013) then extended this model combining texture features with decision tree and SVM classifiers increasing to an F-measure score of 0.76. (Nateghi et al., 2014) omit non-mitosis candidates by a cast function and by minimization using Genetic Optimization, before co-occurrence, run-length matrices and Gabor features are extracted from the rest of candidates to classify mitosis with SVM, achieving an F-score of 0.78 [23].

Most of the latest most-efficient machine algorithms for mitosis detection have been deep learning-based since it is hard to manually design meaningful and discriminative features well enough to separate a mitosis from a non-mitosis due to the variation and complexity of the shapes. With a large number of labeled training images feature extraction is left to the DNN which is optimized using mini-batch gradient descent. Low level layers learn the low level features of the training images, while high level features are learned by the deep layers. Although data-driven models are more computationally expensive, they have the advantage of being able to detect features that cannot be represented by handcrafted features.

For example, (Cirean et al., 2013) used a feed-forward net made of suc-

cessive pairs of convolutional and max-pooling layers, followed by several fully connected layers [6]. This approach achieved an F-measure score of 0.78, the winning score in the ICPR 2012 contest summarized in [30], yet it requires multiple days for training and making it less clinically applicable. Additionally, (Albayrak et al., 2016) developed a CNN which uses a combination of PCA and LDA dimension reduction methods for regularization and dimension reduction process before classification of mitosis by an SVM [1]. (Chen et al., 2016) propose a method combining a deep cascaded CNN to locate mitosis candidates and a discrimination model using transferred cross-domain knowledge, achieving an F1 score of 0.79 on ICPR 2012 [5]. (Wu et al., 2017) used deep fused fully convolutional neural network modified to combine low and high level layer together using to reduce over-fitting [41]. (Xue & Ray, 2018) train a CNN to predict and encode a compressed vector of fixed dimension formed by random projections of the output pixels, achieving state-of-the-art results [42]. (Wahab et al., 2019) used a pre-trained CNN for segmentation and then a Hybrid-CNN for mitosis classification, achieving an F-score of 0.71 [39].

There has also been a number attempts to combine the domain and learned characteristics to exploit the benefits of each. For example, (Wang et al., 2014) present a cascaded approach separately extracting each type of features for each sub-image region, achieving an F-score of 0.73 on ICPR 2012. Regions where the two individual classifiers disagree are further classified by a third classifier, and the final prediction score is a weighted average of the outputs of all classifiers [40]. (Malon et al., 2013) combines color, texture, and shape features from segmented mitosis regions with extracted by convolutional neural networks (CNN), achieving an 0.66 F-score [22].

Since mitosis counting is more of an object detection problem, a number of region-based CNN approaches have been proposed, achieving scores which exceed those of standard deep learning. (Cirean et al., 2013), the winners of the ICPR 2012 contest first modeled the problem using a sliding window version of CNN. (Li et al., 2018) developed a three stage region-based CNN to run only on a CPU. This included a coarse candidate extractor to classify each pixel as mitosis or not, a fine candidate extractor that uses a CNN to output a probability map of a mitosis, and a final predictor with a CNN at a higher threshold [20]. (Rao, 2018) uses a region based convolutional neural network (RCNN) which beat all three contest winners scores when trained on all three datasets from each contest [26]. (Li et al., 2018) uses multi-stage deep learning based on Faster RCNN in combination with a verification model using residual networks to distinguish false positives from detections, achieving an F-score of 0.83 on the 2012 MITOSIS dataset and 0.44 on the 2012 dataset. A segmentation component is included to estimate the region of mitosis when weak labels are given for training [17].

4 Methods

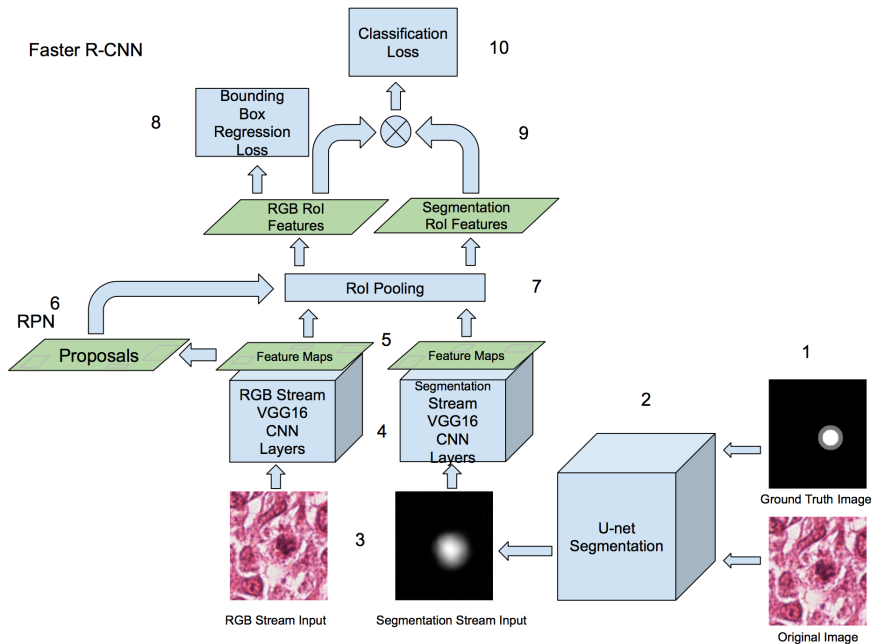


Figure 1: Multi-Stream Faster R-CNN Training. Segmented images are produced by first testing images on U-net are used to add additional features on the second stream. The last layer of the CNN outputs anchors with multiple scales and aspect ratios which are used for the RPN to propose regions. Only the last layer of the RGB stream CNN is used as input to the RPN, so both streams share these region proposals. Then the ROI pooling layer selects spatial features from each stream and outputs a fixed length feature vector for each proposal. The RoI features from the RGB stream alone are used for the final mitosis bounding box location prediction. Then, Bilinear ROI pooling is used to obtain spatial co-occurrence features from both streams [45].

4.1 U-net Segmentation

Part of the process of preparing the data for training Faster R-CNN includes applying segmentation to the images for application to the segmentation stream. This was done with a U-net, as shown in the parts 1 and 2 of the block diagram of Figure 1 which lays out the training process. This a 23-layer network is based on the work of (Ronneberger et al., 2015) [28], winner of ISBI Challenges in biomedical image segmentation and cell tracking [2]. The down-sampling side of the U doubles the number of features in each step while the up-sampling side halves features in each step. The contracting path uses repeated pairs of 3x3

un-padded convolutions to capture image context before a rectified linear unit (ReLU), followed by a 2x2 max pooling operation with stride two. The symmetric expanding path helps to achieve localization and uses a 2x2 convolution and two 3x3 convolutions each followed by a ReLU.

This image segmentation network requires ground truth images for training. In other words, a black image with a white mask in the area of localization needs to be fed to the network, simultaneously, with each RGB (red, green, blue color scale) image subsection (described in 5.1), as shown in Figure 1 labeled part 1. Ground truth data for the segmentation network is created for each image subsection in the training set by drawing a square of black pixels the same size as each image subsection, with a white circle of pixels in the same location of mitosis using the annotated coordinates of the mitosis location (provided with the dataset.) Images input into U-net must also be slightly downsized to avoid padding issues. U-net is then trained for 80 iterations on half of the Faster R-CNN training set (consisting of only the Aperio scanner images and their corresponding ground truth images), while it is tested on the images from both scanners to create the full set of segmented training data for the segmentation stream input of Faster R-CNN. It is important that at least half of the test data for U-net is not in the training set since the actual test images for the full multi-stream network will not be in the training set of U-net. This avoids overfitting U-net to allow for imperfections in segmented training data.

4.2 Multi-Stream CNN

The framework presented in parts labeled 3 through 10 of Figure 1 is a multi-stream version of the Faster R-CNN object detection network [27]. In this work, the network is adapted to classify regions of interest having a mitosis, instead of classifying actual physical objects. One stream takes an input of the segmented image map while the other takes an input of the original RGB image. In part 3, the segmented training data output from U-net is used for input to the segmentation stream of the multi-stream Faster-RCNN. Original images with all three color channels are used again in Faster R-CNN as input to the RGB stream. The purpose of the segmentation stream is to provide additional evidence of mitosis locations by emphasizing the segmented features picked up by U-net. The base convolutional neural network (CNN) in part 4 is a VGG-16 network pre-trained on ImageNet [7]. Around 9 boxes with different scales and aspect ratios are generated from each position (anchor) of the output feature map produced in the last layer of the CNN (part 5). This produces thousands of boxes that can be used for region proposals generated by the Region Proposal Network (RPN) during training (part 6.)

4.3 Region Proposal Network

The purpose of the RPN is to pre-check and refine which locations before sending them to the detection and classification network to finalize them (section). It is a simple 3 layer convolutional network which has one layer that is fed into

two sibling fully connected layers used for classification and bounding box regression, respectively. Each region surrounding an anchor is regressed to the tighten and center around the position most likely to be an object location [15]. During training, proposals that overlap the ground-truth objects with an Intersection over Union (IoU) greater than 0.5 are considered foreground, while those with a 0.1 IoU or less are considered background objects, while the rest are ignored. A fixed number of proposals is then output as this class probability representing the *objectness* score and a refined estimation of its rectangular coordinates [15]. Non-maximum suppression (NMS) is used to ensure there is not an overlap of the proposed regions, retaining the overlapping boxes with the highest probabilities. Check this from Deep-mitosis:

The loss for the RPN network is defined as below [27].

$$L_{RPN}(g_i, f_i) = \frac{1}{N_{cls}} \sum_i L_{cls}(g_i, g_i^*) + \lambda \frac{1}{N_{reg}} \sum_i g_i^* L_{reg}(f_i, f_i^*)$$

- g_i represents the probability of anchor i being a mitosis in a mini batch,
- g_i^* is the ground-truth label for anchor i being a mitosis
- f_i, f_i^* are the four dimensional bounding box coordinates for anchor i and the ground-truth, respectively
- L_{cls} denotes cross entropy loss for RPN network, and L_{reg} denotes smooth L_1 loss for regression
- N_{cls} denotes the size of a mini-batch, and N_{reg} is the number of anchor locations.
- λ is a hyper-parameter to balance the two losses

Note, that the arrow pointing towards the RPN in Figure 1 is directed from the last-layer feature map in the Faster R-CNN RGB stream, because the RPN shares convolutional features with this CNN *only*, as it is shown to be most efficient for measuring color changes [44].

4.4 Region of Interest Pooling

The Region of Interest (RoI) pooling layer (part 7) takes all of the arbitrary sized spatial feature maps provided by the RPN and converts them into a fixed size feature vector using max-pooling [32]. The segmentation and RGB streams share the RoI pooling layer, so each of these two CNN feature maps are pooled with indices and coordinates from the RGB RoI.

4.5 Detection Network

The Detection Network (also known as R-CNN) further classifies and regresses the boxes against the actual mitosis regions for final prediction beyond just foreground and background objects (as in the RPN)

4.5.1 Bounding Box Regression

Only the RGB stream RoI features are used to finalize object coordinates because they perform better than segmentation features in the RPN [45]. This is for bounding box regression using smooth L_1 loss as shown in part 8 and the equations below.

4.5.2 Bilinear Pooling

Compact bilinear pooling is used in part 9 of Figure 1 to fuse the co-occurrence of features from both streams while maintaining the spatial location information [8]. The RoI are combined using a two stream of CNN, and the output is equal to $f_{RGB}^T f_{seg}$, where f_{RGB} is the RoI of the RGB stream and f_{seg} is the RoI of the segmentation stream [14].

4.5.3 Classification

The final predicted classes are output from the network’s fully connected and soft-max layers using sparse cross entropy loss (part 10).

4.6 Total Loss Function

The backward propagated signals from the RPN loss and the Fast R-CNN loss are combined for shared layers [9], so the total network loss function is the sum of all 3 of the loss components as shown below:

$$L_{total} = L_{RPN} + L_{mitosis}(f_{RGB}, f_{seg}) + L_{bbox}(f_{RGB})$$

where

- L_{total} denotes total loss
- L_{RPN} denotes the RPN loss
- $L_{mitosis}$ denotes the final cross entropy classification loss (based on the output of multi-stream pooling)
- L_{bbox} denotes the final bounding box regression loss
- f_{RGB} represents the RoI from the RGB stream
- f_{seg} represents the RoI from the segmentation stream

5 Experiments

5.1 Training Data Preparation

The multi-stream model was first trained on a subset of the MITOS-ATYPIA-14 contest dataset [30]. Image data for this contest was obtained with the Aperio Scanscope XT and the Hamamatsu Nanozoomer 2.0-HT slide scanners and

stained with standard hematoxylin and eosin (H&E) dyes. The X40 resolution training set provided consists of 1,136 labeled 1539×1376 pixel HPF frames, containing 749 labeled mitotic cells in 22 compressed files. Image annotations for the coordinates of the center pixel each mitosis are made by two senior pathologists, where if one disagrees a third will give the final say. According to the contest evaluation criteria, a correct detection is the one that lies within 32 pixels from this centroid of the ground truth mitosis. Contestants are ranked according to their F-measure, which is a harmonic mean of precision and recall (sensitivity), as described below.

$$F - measure = \frac{2 \cdot (precision \cdot sensitivity)}{(precision + sensitivity)} \quad (1)$$

The precision measures how accurate the predictions are using the percentage of the correct predictions out of the total. It is calculated using the FP which represents the number of false positive predictions, and TP which is the number of true positive predictions, as shown below:

$$Precision = \frac{TP}{FP + TP} \quad (2)$$

The recall measures how well all the positives are found in the test set, where FN is the number of false negatives (those ground truths which were not detected), as shown below

$$Recall = \frac{TP}{FN + TP} \quad (3)$$

One of the official training set files was designated for testing (A03, consisting of 96 images containing 135 mitosis), which is comparable to other groups who tested on this data. On the other hand this is a smaller training and test set than contestants used, since annotations are only provided for the training data. HPF slides were converted from TIFF to JPEG image files, before being cropped into 16 equally sized subsections. Next, the subsections were expanded to 1.7 times the original image size to increase the mitosis size to be large enough compared to the smallest detectable object size of Faster RCNN.

6 Results

When the network was tested on the MITOS-ATYPIA-2014 dataset, an F-measure score of 0.507 was obtained. This is already significantly higher than contest winners score of 0.356, and our network was trained on a smaller portion of the training set with little data augmentation to the training data. Beyond the contest winners this is also higher than a recent similar tests on this dataset using deep learning and achieving scores of 0.437 and 0.442 [18].

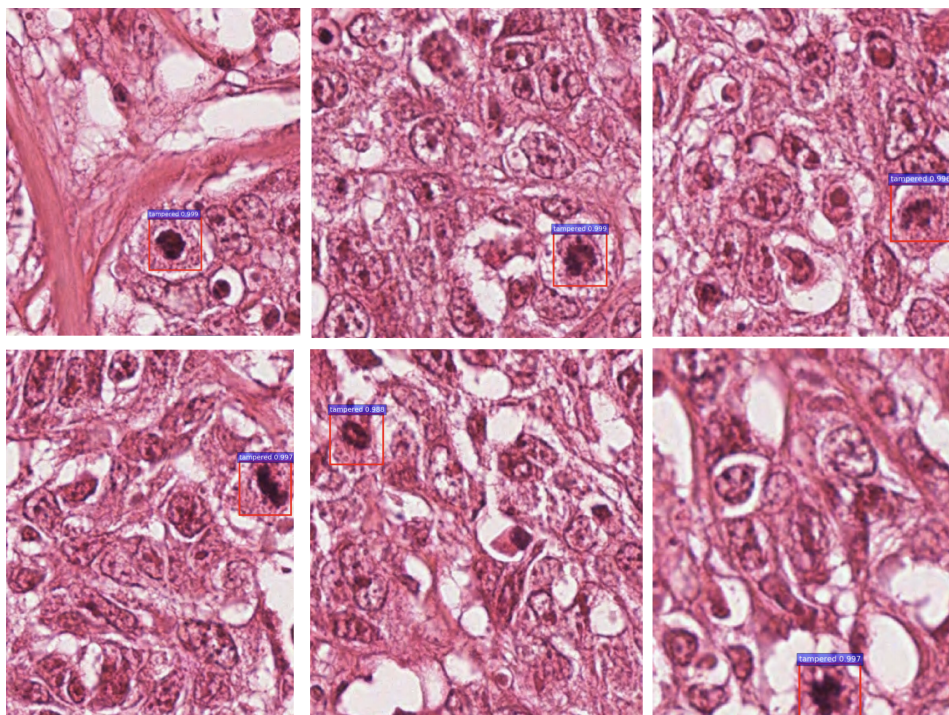


Figure 2: Examples of Predictions with Multi-stream model (with K-means) on a Subset of MITOS-ATYPIA-14 Data

7 Conclusion

It will next be tested in combination with multiple or alternate methods in a multilinear model with 2 or more separate segmentation streams to find which method provides the best information. There are also various methods of preparing the training images, such as rotating, mirroring, resizing, using a sliding window, estimating the mitosis bounding boxes (more precisely than using the centroid alone) and cropping out images containing mitosis cross boundaries can then help provide more training samples to the network and significantly improve accuracy when the size of the training data is small [18] [19]. Modifications to the network layers and parameters will likely lead to additional improvements [31] [17].

References

- [1] A. Albayrak and G. Bilgin. Mitosis detection using convolutional neural network based features. In *2016 IEEE 17th International Symposium*

- on *Computational Intelligence and Informatics (CINTI)*, pages 000335–000340, Nov 2016.
- [2] Ignacio Arganda-Carreras, Srinivas C. Turaga, Daniel R. Berger, Dan Cirean, Alessandro Giusti, Luca M. Gambardella, Jrgen Schmidhuber, Dmitry Laptev, Sarvesh Dwivedi, Joachim M. Buhmann, Ting Liu, Mojtaba Seyedhosseini, Tolga Tasdizen, Lee Kamensky, Radim Burget, Vclav Uher, Xiao Tan, Changming Sun, Tuan D. Pham, Erhan Bas, Mustafa G. Uzunbas, Albert Cardona, Johannes Schindelin, and H. Sebastian Seung. Crowdsourcing the creation of image segmentation algorithms for connectomics. *Frontiers in Neuroanatomy*, 9:142, 2015.
- [3] Akinfenwa. Atanda, Mohammed. Imam, Ali. Umar, Ibrahim. Yusuf, and Shamsu. Bello. Audit of nottingham system grades assigned to breast cancer cases in a Teaching Hospital. *Annals of Tropical Pathology*, 8(2):104–107, 2017.
- [4] Maschenka C. A. Balkenhol, Peter Bult, David Tellez, Willem Vreuls, Pieter C. Clahsen, Francesco Ciompi, and Jeroen A. W. M. van der Laak. Deep learning and manual assessment show that the absolute mitotic count does not contain prognostic information in triple negative breast cancer. *Cellular Oncology*, 42(4):555–569, Aug 2019.
- [5] Hao Chen, Qi Dou, Xi Wang, Jing Qin, and Pheng-Ann Heng. Mitosis detection in breast cancer histology images via deep cascaded networks. In *Proceedings of the Thirtieth AAAI Conference on Artificial Intelligence*, AAAI’16, pages 1160–1166. AAAI Press, 2016.
- [6] Dan Cirean, Alessandro Giusti, Luca Maria Gambardella, and Jrgen Schmidhuber. Mitosis detection in breast cancer histology images with deep neural networks. volume 16, pages 411–8, 09 2013.
- [7] J. Deng, W. Dong, R. Socher, L.-J. Li, K. Li, and L. Fei-Fei. ImageNet: A Large-Scale Hierarchical Image Database. In *CVPR09*, 2009.
- [8] Yang Gao, Oscar Beijbom, Ning Zhang, and Trevor Darrell. Compact bilinear pooling, 2015.
- [9] Ross B. Girshick. Fast R-CNN. *CoRR*, abs/1504.08083, 2015.
- [10] C. Huang and H. Lee. Automated mitosis detection based on exclusive independent component analysis. In *Proceedings of the 21st International Conference on Pattern Recognition (ICPR2012)*, pages 1856–1859, Nov 2012.
- [11] S. Huh, D. F. E. Ker, R. Bise, M. Chen, and T. Kanade. Automated mitosis detection of stem cell populations in phase-contrast microscopy images. *IEEE Transactions on Medical Imaging*, 30(3):586–596, March 2011.

- [12] A. M. Khan, H. El-Daly, and N. M. Rajpoot. A gamma-gaussian mixture model for detection of mitotic cells in breast cancer histopathology images. In *Proceedings of the 21st International Conference on Pattern Recognition (ICPR2012)*, pages 149–152, Nov 2012.
- [13] Daisuke Komura and Shumpei Ishikawa. Machine learning methods for histopathological image analysis. *Computational and Structural Biotechnology Journal*, 16:34 – 42, 2018.
- [14] Shu Kong and Charless C. Fowlkes. Low-rank bilinear pooling for fine-grained classification. *CoRR*, abs/1611.05109, 2016.
- [15] Daniel Konig, Michael Adam, Christian Jarvers, Georg Layher, Heiko Neumann, and Michael Teutsch. Fully convolutional region proposal networks for multispectral person detection. In *The IEEE Conference on Computer Vision and Pattern Recognition (CVPR) Workshops*, July 2017.
- [16] Leor Langer, Yoav Binenbaum, Leon Gugel, Moran Amit, Ziv Gil, and Shai Dekel. Computer-aided diagnostics in digital pathology: automated evaluation of early-phase pancreatic cancer in mice. *International journal of computer assisted radiology and surgery*, 10, 10 2014.
- [17] Chao Li, Xinggang Wang, Wenyu Liu, and Longin Jan Latecki. Deepmitosis: Mitosis detection via deep detection, verification and segmentation networks. *Medical Image Analysis*, 45:121 – 133, 2018.
- [18] Chao Li, Xinggang Wang, Wenyu Liu, and Longin Jan Latecki. Deepmitosis: Mitosis detection via deep detection, verification and segmentation networks. *Medical Image Analysis*, 45:121 – 133, 2018.
- [19] Chao Li, Xinggang Wang, Wenyu Liu, Longin Jan Latecki, Bo Wang, and Junzhou Huang. Weakly supervised mitosis detection in breast histopathology images using concentric loss. *Medical Image Analysis*, 53:165 – 178, 2019.
- [20] Yuguang Li, Ezgi Mercan, Stevan Knezevitch, Joann G. Elmore, and Linda G. Shapiro. Efficient and accurate mitosis detection - a lightweight rcnn approach. In *ICPRAM*, 2018.
- [21] A. Liu, K. Li, and T. Kanade. Mitosis sequence detection using hidden conditional random fields. In *2010 IEEE International Symposium on Biomedical Imaging: From Nano to Macro*, pages 580–583, April 2010.
- [22] Christopher Malon and Eric Cosatto. Classification of mitotic figures with convolutional neural networks and seeded blob features. In *Journal of pathology informatics*, 2013.
- [23] R. Nateghi, H. Danyali, M. SadeghHelfroush, and F. P. Pour. Automatic detection of mitosis cell in breast cancer histopathology images using genetic algorithm. In *2014 21th Iranian Conference on Biomedical Engineering (ICBME)*, pages 1–6, Nov 2014.

- [24] Emad Rakha, Jorge Reis-Filho, Frederick Baehner, David Dabbs, Thomas Decker, Vincenzo Eusebi, Stephen Fox, Shu Ichihara, Jocelyne Jacquemier, Sr Lakhani, Jos Palacios, Andrea Richardson, Stuart Schmitt, Fernando Schmitt, Puay-Hoon Tan, Gary Tse, Sunil Badve, and Ian Ellis. Breast cancer prognostic classification in the molecular era: the role of histological grade. *Breast cancer research : BCR*, 12:207, 07 2010.
- [25] Siddhant Rao. MITOS-RCNN: A novel approach to mitotic figure detection in breast cancer histopathology images using region based convolutional neural networks. *CoRR*, abs/1807.01788, 2018.
- [26] Siddhant Rao. Mitos-rcnn: Mitotic figure detection in breast cancer histopathology images using region based convolutional neural networks. *International Journal of Medical and Health Sciences*, 12(10):514 – 520, 2018.
- [27] Shaoqing Ren, Kaiming He, Ross B. Girshick, and Jian Sun. Faster R-CNN: towards real-time object detection with region proposal networks. *CoRR*, abs/1506.01497, 2015.
- [28] Olaf Ronneberger, Philipp Fischer, and Thomas Brox. U-net: Convolutional networks for biomedical image segmentation, 2015.
- [29] L. Roux. Mitos-atypia-14 - grand challenge, 2014.
- [30] Ludovic. Roux, Daniel. Racoceanu, Nicolas. Lomnie, Maria. Kulikova, Humayun. Irshad, Jacques. Klossa, Frdrique. Capron, Catherine. Genestie, Gilles. Naour, and Metin. Gurcan. Mitosis detection in breast cancer histological images An ICPR 2012 contest. *Journal of Pathology Informatics*, 4(1):8, 2013.
- [31] Monjoy Saha, Chandan Chakraborty, and Daniel Racoceanu. Efficient deep learning model for mitosis detection using breast histopathology images. *Computerized Medical Imaging and Graphics*, 64, 12 2017.
- [32] Pierre Sermanet, David Eigen, Xiang Zhang, Michael Mathieu, Rob Fergus, and Yann LeCun. Overfeat: Integrated recognition, localization and detection using convolutional networks, 2013.
- [33] C. Sommer, L. Fiaschi, F. A. Hamprecht, and D. W. Gerlich. Learning-based mitotic cell detection in histopathological images. In *2012 21st International Conference on Pattern Recognition (ICPR 2012)*, pages 2306–2309, Los Alamitos, CA, USA, nov 2012. IEEE Computer Society.
- [34] F. Boray Tek. Mitosis detection using generic features and an ensemble of cascade adaboosts. In *Journal of pathology informatics*, 2013.
- [35] Thana Tosta, Leandro A. Neves, and Marcelo Zanchetta do Nascimento. Segmentation methods of he-stained histological images of lymphoma: A review. *Informatics in Medicine Unlocked*, 9, 05 2017.

- [36] M. Veta, P. J. van Diest, and J. P. W. Pluim. Detecting mitotic figures in breast cancer histopathology images. In Metin N. Gurcan and Anant Madabhushi, editors, *Medical Imaging 2013: Digital Pathology*, volume 8676, pages 70 – 76. International Society for Optics and Photonics, SPIE, 2013.
- [37] Mitko Veta, Paul J. van Diest, Mehdi Jiwa, Shaimaa Al-Janabi, and Josien P. W. Pluim. Mitosis counting in breast cancer: Object-level interobserver agreement and comparison to an automatic method. *PLoS ONE*, 11(8), 8 2016.
- [38] Mitko Veta, Paul J. van Diest, Stefan M. Willems, Haibo Wang, Anant Madabhushi, Angel Cruz-Roa, Fabio A. González, Anders Boesen Lindbo Larsen, Jacob S. Vestergaard, Anders B. Dahl, Dan C. Ciresan, Jürgen Schmidhuber, Alessandro Giusti, Luca Maria Gambardella, F. Boray Tek, Thomas Walter, Ching-Wei Wang, Satoshi Kondo, Bogdan J. Matuszewski, Frédéric Precioso, Violet Snell, Josef Kittler, Teófilo Emídio de Campos, Adnan Mujahid Khan, Nasir M. Rajpoot, Evdokia Arkoumani, Mian-gela M. Lacle, Max A. Viergever, and Josien P. W. Pluim. Assessment of algorithms for mitosis detection in breast cancer histopathology images. *CoRR*, abs/1411.5825, 2014.
- [39] Noorul Wahab, Asifullah Khan, and Yeon Soo Lee. Transfer learning based deep cnn for segmentation and detection of mitoses in breast cancer histopathological images. *Microscopy (Oxford, England)*, 68:216–233, 06 2019.
- [40] Haibo Wang, Angel Cruz Roa, Ajay N. Basavanahally, Hannah L. Gilmore, Natalie Shih, Mike Feldman, John Tomaszewski, Fabio Gonzalez, and Anant Madabhushi. Mitosis detection in breast cancer pathology images by combining handcrafted and convolutional neural network features. *Journal of Medical Imaging*, 1(3):1 – 8, 2014.
- [41] Boqian Wu, Tasleem Kausar, Qiao Xiao, Mingjiang Wang, Wenfeng Wang, Binwen Fan, and Dandan Sun. Ff-cnn: An efficient deep neural network for mitosis detection in breast cancer histological images. In María Valdés Hernández and Víctor González-Castro, editors, *Medical Image Understanding and Analysis*, pages 249–260, Cham, 2017. Springer International Publishing.
- [42] Yao Xue and Nilanjan Ray. Cell detection with deep convolutional neural network and compressed sensing. *ArXiv*, abs/1708.03307, 2017.
- [43] Robin Yancey. Machine learning methods for image tampering detection, 2019. SMI Conference.
- [44] Robin Elizabeth Yancey. Bilinear faster RCNN with ELA for image tampering detection. *CoRR*, abs/1904.08484, 2019.

- [45] Peng Zhou, Xintong Han, Vlad I. Morariu, and Larry S. Davis. Learning rich features for image manipulation detection. *CoRR*, abs/1805.04953, 2018.